

Nuclear Magnetic Resonance in KMnF_3 R. G. SHULMAN AND K. KNOX
Bell Telephone Laboratories, Murray Hill, New Jersey

(Received February 12, 1960)

The nuclear magnetic resonance of fluorine in KMnF_3 has been studied and hyperfine interactions between the fluorine nucleus and the magnetic electrons measured. The values are $A_s = (16.26 \pm 0.4) \times 10^{-4} \text{ cm}^{-1}$ and $(A_s - A_\pi) = (0.17 \pm 0.1) \times 10^{-4} \text{ cm}^{-1}$. These values correspond to $(0.52 \pm 0.02)\%$ $2s$ and $(0.18 \pm 0.1)\%$ $2p$ character for the unpaired electron. The implications of these results in terms of the σ and π bonding in this compound are discussed. By a comparison with hyperfine interactions measured in recent paramagnetic resonance studies of $\text{KMgF}_3:\text{Mn}^{+2}$ the amount of distortion in the mixed crystal is estimated. An antiferromagnetic transition is observed at 88.5°K .

INTRODUCTION

NUCLEAR magnetic resonance studies¹ of fluoride nuclei in magnetic crystals have shown the presence of large internal magnetic fields at the nuclei. These fields have shifted the nuclear resonance and have determined the line widths and spin-lattice relaxation times. They have been shown to include hyperfine interactions as well as the dipole fields. The dominant component of the hyperfine interaction has been shown to be isotropic while the smaller anisotropic fields include large contributions from the dipole interaction. The hyperfine interactions have been explained by unpaired spins in the fluoride ion orbitals—unpaired $2s$ electrons considered as the origin of the isotropic effects and unpaired $2p$ electrons as responsible for the anisotropic interactions. Detailed interpretations of the hyperfine interactions in terms of spin densities in particular atomic orbitals requires accurate knowledge about the directional character of the wave functions involved in the interaction between the fluoride ion and the surrounding magnetic electrons. In MnF_2 ¹ the fluoride ion's environment has the symmetry C_{2v} while the environment of manganese is D_{2h} . This low symmetry introduces uncertainty into the direction of the orbitals containing unpaired spins and complicates the interpretation in terms of fluoride ion orbitals.

In the interests of interpreting the nuclear resonance shifts in terms of spin density in atomic orbitals it is desirable to study a crystal of high symmetry. The cubic crystal of KMnF_3 , ideal perovskite in structure² was studied for these reasons.

EXPERIMENTAL

KMnF_3 is one of a series of mixed salts KXF_3 where $\text{X} = \text{Cr, Mn, Fe, Co, Ni, Cu, Zn, or Mg}$. They have perovskite-like structures, as shown in Fig. 1, with the divalent metal at the body-centered position, potassium at the cube corners and three fluorides at the face-centered positions. In the cubic KMnF_3 , the symmetry is such that each manganese ion at a site of symmetry O_h is surrounded by a regular octahedron of fluorides

while each fluoride at a site whose symmetry is D_{4h} has two colinear manganese neighbors as illustrated in Fig. 1. There are three unique fluorine environments identical except for their orientations with respect to the three Cartesian coordinates. The internal magnetic fields in this crystal at the fluorine nuclei come from magnetic interactions with the manganese ions. To the extent that these interactions are anisotropic they have the angular dependence $(3 \cos^2 \theta - 1)$ where θ is the angle between the direction of electron polarization and the internuclear radius. It can be seen from this consideration that for an arbitrary orientation of an external magnetic field there are three distinct fluorine sites. This applies to the paramagnetic state where the electrons with isotropic g factors are partially polarized by the external magnetic field. For H_0 in (110) there are in general only two distinct fluorine sites and consequently two fluorine resonance fields while for $H_0 \parallel [111]$ all fluorines are identical and there is one resonance. Our measurements in the paramagnetic state were made with H_0 in the (110) plane so that in general there are two resonances observed except for $H_0 \parallel [111]$. A spherical sample $\sim 6 \text{ mm}$ diameter was cut from a single crystal² of KMnF_3 , oriented by x-rays and cemented with silica cement to a single crystal

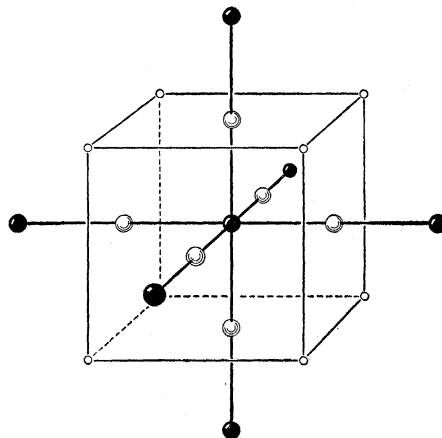


FIG. 1. Perovskite structure of KMnF_3 . The Mn^{++} ion at the body centered position with site symmetry O_h is surrounded by six fluoride ions. Each fluoride ion is colinear with two Mn^{++} ions.

¹ R. G. Shulman and V. Jaccarino, Phys. Rev. **108**, 1219 (1957).

² K. Knox (to be published).

sapphire rod with a $[110]$ direction parallel to the axis of the rod. For the room temperature measurements shown in Fig. 2 a Varian Associates fixed frequency induction spectrometer operating at 60.000 Mc/sec was used, the magnetic field being varied to bring about the resonance condition. A Varian variable frequency spectrometer was used for the 90°K measurements shown in Fig. 3. The magnetic field was measured by observing the Li^7 nuclear resonance in a water solution of LiCl using a modified³ Pound-Knight spectrometer. Two resonance lines for KMnF_3 were clearly resolved under these conditions and a recorder trace of the absorption derivative is shown in Fig. 4 for $H_0 \parallel [001]$ which is the point of greatest splitting. As can be seen from the trace the two lines are not equally wide, but rather the more displaced line is broader. The less displaced, higher field, resonance corresponds to two identical fluorine sites along $[100]$ and $[010]$. Its width between derivative extrema is 17 ± 1 gauss corre-

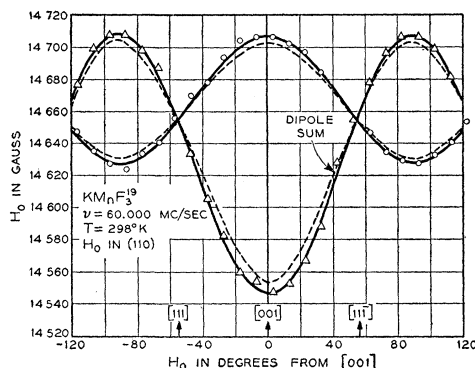


FIG. 2. The resonance field H_0 versus the angle between H_0 and $[001]$ for H_0 in (110) plane at 298°K and $\nu = 60.000$ Mc/sec. The dashed curve represents the dipole sum whose numerical value for this configuration is given by Eq. (7).

sponding for this Lorentzian shape to $T_2 = 2.4 \times 10^{-6}$ second. The weaker resonance at a lower field has contributions from one fluorine site along $[001]$, and its integrated intensity is $\sim \frac{1}{2}$ that of the higher field line. Its width between extrema is 22.5 gauss so that $T_2 = 1.8 \times 10^{-6}$ second. The origin of these line widths will be discussed in the next section in terms of exchange narrowing^{4,5} of the hyperfine interactions.

When we started this investigation the only available information concerning the antiferromagnetic ordering in KMnF_3 was in a short note⁶ by Martin, Nyholm, and Stephenson in which they briefly reported susceptibility measurements between 90°–400°K on several of these complex fluorides. KNiF_3 had a susceptibility

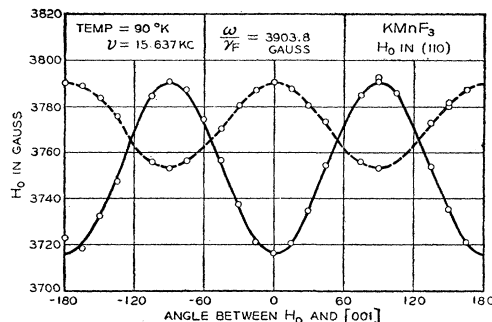


FIG. 3. Similar to Fig. 2 but at 90°K and $\nu = 15.637$ Mc/sec.

maximum at 275°, KCoF_3 at 135°K, KFeF_3 at 115°K, and, although it was indicated that KMnF_3 was antiferromagnetic, the results were incomplete.

In Fig. 5 we have plotted the NMR shifts measured with $H_0 \parallel [111]$ at different temperatures between 90°K and 300°K. It has been shown in the past¹ that these NMR shifts in paramagnetic materials are proportional to the expectation value of the electron spin $\langle S \rangle$ which is a function of temperature. For Mn^{++} salts such as KMnF_3 in which $\langle S \rangle$ is proportional to the susceptibility χ , as is shown below, we expect the shifts to be proportional to the susceptibility. When a comparison is made between the susceptibility measurements⁷ and the NMR shifts they have the same temperature dependence within the experimental errors.

At 90°K the resonance pattern had the same symmetry as it did at higher temperatures as shown in a comparison of Fig. 2 and Fig. 3. However at 77°K a different pattern was observed in our somewhat cracked single crystal sphere. The lines were quite broad, rather difficult to measure exactly, but plainly did not have the same angular dependence as they had above 90°K. This indicated that a transition to an ordered state had occurred between 90°K and 77°K. This would be consistent with the published results⁶ stating that T_N was

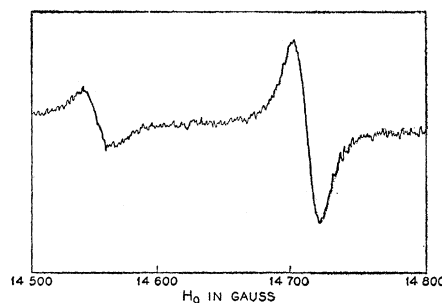


FIG. 4. Recorder trace of F^{19} resonance derivative with $H_0 \parallel [001]$ at $T = 298^\circ\text{K}$, $\nu = 60.000$ Mc/sec; modulation is 8.9 gauss and output time constant is 0.8 second.

³ J. M. Mays, H. R. Moore, and R. G. Shulman, *Rev. Sci. Instr.* **29**, 300 (1958).

⁴ T. Moriya, *Progr. Theoret. Phys. (Kyoto)* **16**, 23, 641 (1956).

⁵ P. W. Anderson and P. R. Weiss, *Revs. Modern Phys.* **25**, 269 (1953).

⁶ R. L. Martin, R. S. Nyholm, and N. C. Stephenson, *Chem. & Ind. (London)* **1956**, 83.

⁷ The susceptibility of KMnF_3 has recently been measured in three independent experiments. Dr. N. Elliott and Dr. R. L. Martin have kindly provided us with their unpublished results. While waiting for their data we made an independent measurement at selected temperatures in collaboration with Dr. M. A. Gilleo. In the text we only use the value of χ_m at 298°K.

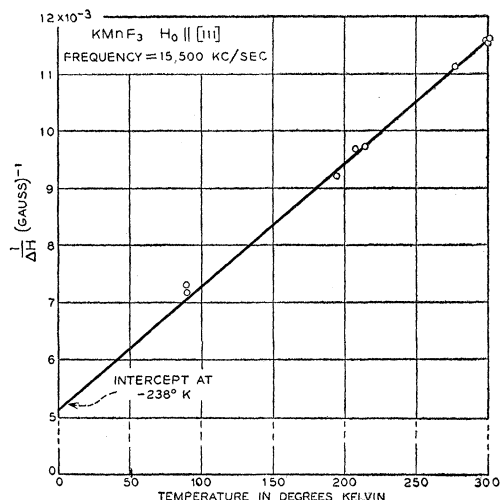


FIG. 5. In this diagram ΔH is the displacement of the F^{19} resonance from its unshifted position of ω/γ_N . The susceptibility should be proportional to ΔH and in fact the experimental values of $1/\Delta H$ plotted can be fitted quite well to the susceptibility data⁷ of N. Elliot and R. L. Martin.

$<100^\circ\text{K}$ and also with our measured NMR shifts. These measured shifts, being proportional to the susceptibility, give a straight line of $1/\Delta H$ versus T with an intercept of -238°K (Fig. 5). Corresponding to these data the susceptibility, which was then not available in this temperature region, should approximately follow a Curie-Weiss law of the form $\chi = [C/(T + \Theta)]$ where $\Theta = 238^\circ\text{K}$. Obviously the data were taken at temperatures too close to T_N to expect the Curie-Weiss law to be valid, since the first term in the expansion of χ in powers of $1/T$ only predominates for $T \gg T_N$. However in a qualitative way the data indicated first that the ordered state would be antiferromagnetic (because Θ was positive) and second that $90^\circ\text{K} > T_N > 77^\circ\text{K}$ was reasonable. In order to observe the transition a single crystal sample was placed in liquid oxygen with $H_0 \parallel [111]$ so that one resonance line was observed as the temperature was lowered by pumping on the oxygen. The intensity of the signal was observed to vary with temperature in the manner shown in Fig. 6. In the region of 88.5° a transition in the resonance intensity occurred over a temperature interval of about one degree. Measurements were made by sweeping back and forth through the resonance line as the temperature was lowered. The three points indicated by crosses in Fig. 6 were taken as the temperature was raised, the others while it was lowered. Whether they indicate hysteresis at T_N as observed⁸ in oxides by F. J. Morin, or merely reflect a temperature lag of the thermocouple fastened slightly above the sample is not certain. Our preliminary report⁹ of

⁸ F. J. Morin (private communication) and Phys. Rev. Letters **3**, 34 (1959).

⁹ R. G. Shulman, K. Knox, and B. J. Wyluda, Bull. Am. Phys. Soc. **4**, 166 (1959).

$T_N \approx 88.3^\circ\text{K}$ has been confirmed by recent susceptibility measurements.¹⁰

Measurements have been made on powder samples of KCoF_3 and KNiF_3 . Both showed paramagnetic NMR shifts at 300°K which we could not measure accurately because the resonances were very broad and showed structure. When the KNiF_3 was observed at 77°K the structure had disappeared and a broad symmetrical resonance was observed. The transition between these two patterns in KNiF_3 occurred in the vicinity of 250°K . Martin, Nyholm, and Stephenson⁶ reported a susceptibility maximum at 275°K . Considering that these KNiF_3 experiments are only preliminary the agreement seems reasonable and the antiferromagnetic transition of KNiF_3 is in this region.

From the F^{19} resonance data in the ordered state it is in principle possible to determine the antiferromagnetic ordering. Work in this region was made very difficult by the broad lines observed. However it was clear that the large internal fields which would be expected from the isotropic interaction with two Mn^{++} neighbors whose spin alignments were parallel would have shifted the F^{19} resonance in zero magnetic field¹¹ to several hundred megacycles. Since the lines were on the average not shifted this far, but only displaced up and down in field from the normal position of ω/γ_N , the absence of large isotropic shifts could be explained by each F^{19} having its two neighboring Mn^{++} spins arranged antiparallel. Our results are therefore consistent with the findings of Scatturin, Corliss, Elliott, and Hastings¹² which have recently become available in which they have established by neutron diffraction measurements just this spin alignment, i.e., every spin has six nearest neighbors whose spins are antiparallel to the first spin. Other recent studies indicate¹³ additional complications in the magnetic structure at 77.3° which should explain our broad observed resonances.

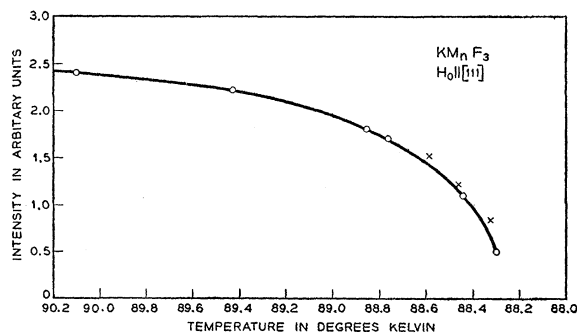


FIG. 6. Intensity of F^{19} resonance line versus temperature showing the rapid decrease of intensity near 88.5°K .

¹⁰ S. Ogawa, J. Phys. Soc. Japan **14**, 1115 (1959).

¹¹ V. Jaccarino and R. G. Shulman, Phys. Rev. **107**, 1196 (1957).

¹² V. Scatturin, L. Corliss, N. Elliott, and J. Hastings (private communication).

¹³ O. Beckman, A. J. Heeger, A. M. Portis, and D. T. Teaney, Bull. Am. Phys. Soc. Ser II, **5**, 188 (1960).

HYPERFINE INTERACTION

As mentioned above, KMnF_3 was investigated because its symmetrical structure allows an unambiguous interpretation of the hyperfine interactions observed in terms of atomic orbitals. The nuclear Hamiltonian has been discussed previously.¹ It can be written

$$H = -\gamma\hbar\mathbf{I}\cdot\mathbf{H} + \sum_j \mathbf{I}\cdot\mathbf{A}_j\cdot\mathbf{S}_j + \sum_j \gamma\hbar\mathbf{I}\cdot\beta\mathbf{g}\cdot\mathbf{S} \frac{(3\cos^2\theta_j - 1)}{r_j^3} \quad (1)$$

where the first term is the nuclear Zeeman energy and the second is the hyperfine interaction with the j th magnetic ion of spin S_j . The dipole interaction with the j th ion whose gyromagnetic ratio is g and which is located at a distance r_j from the nucleus is given by the third term on the right-hand side. Anisotropic dipole fields are functions of θ_j , the angle between the external magnetic field H_0 and r_j . If we make the simplifications permitted by the geometry of KMnF_3 and sum the hyperfine interaction over the two nearest Mn^{++} neighbors we can derive^{1,9} from Eq. (1) the resonance frequency as

$$h\nu = g_N\beta_N(H_0 + H^D) - [A_s + (A_\sigma - A_\pi)(3\cos^2\theta_\sigma - 1)] \times [\langle S_1 \rangle + \langle S_2 \rangle] \quad (2)$$

in which $\langle S_1 \rangle$ and $\langle S_2 \rangle$ refer to the spin expectation value of the two Mn^{++} neighbors. In this expression g_N is the nuclear g factor, β_N the nuclear magneton, and H^D is the dipole field of the Mn^{++} ions which will be defined. Following Tinkham¹⁴ the hyperfine interaction has been considered to consist of an isotropic component A_s and anisotropic components A_σ and A_π . The A_σ interactions arise from unpaired spins in the fluorine p orbitals which lie along the $\text{Mn}^{++}\text{-F}^-$ internuclear radii. The A_π interactions arise from electrons in the p orbitals perpendicular to this direction. Some of the assumptions involved in writing Eq. (2) in this form are discussed more fully in the Appendix. The angle between H_0 and the internuclear radius is θ_σ . It can be seen from Eq. (2) that there are only two independent parameters of the hyperfine interaction, i.e., A_s and $(A_\sigma - A_\pi)$, so that our experiments can only determine these two unknowns. The reason for this is that the magnetic field at the F^{19} nucleus from equal densities of unpaired spins in the three p orbitals can be expressed as a sum of the three spherical harmonics of order $l=1$. Since the sum of this complete set is invariant under any rotation it is clear that the anisotropic terms, by definition direction dependent, must be expressed in terms of the differences of spin density in two of the orbitals as compared with the third. Taking the third orbital to be one of the p_π orbitals

perpendicular to the σ bonds it can be seen from the fourfold symmetry about the σ bond that the two π bonds must be identical. These considerations have been used to simplify Eq. (2). In Eq. (2) the dipole fields H^D are obtained from the expression

$$H^D = \frac{H_0\chi_m}{N} \sum_j \frac{(3\cos^2\theta_j - 1)}{r_j^3} \quad (3)$$

which results from the dipole contribution to Eq. (1) if we substitute

$$\chi_m = \sum_j \frac{\mu_j}{H_0} = \sum_j \left(-\frac{g\beta S_j}{H_0} \right).$$

It has also been assumed that χ_m is isotropic as it should be for KMnF_3 and it has been removed from the summation. The summation over the entire lattice has been performed on the IBM 704.

It is convenient to write the measured NMR shifts as

$$h\nu = g_N\beta_N H_0(1 + \alpha). \quad (4)$$

Substituting these expressions in Eq. (2) for the two resonances observed with $H_0 \parallel [001]$ we have

$$g_N\beta_N(\alpha_{\perp} - H_{\perp}^D/H_0)H_0 = (\chi_m/Ng\beta)[2A_s - 2(A_\sigma - A_\pi)] \quad (5)$$

and

$$g_N\beta_N(\alpha_{\parallel} - H_{\parallel}^D/H_0)H_0 = (\chi_m/Ng\beta)[2A_s + 4(A_\sigma - A_\pi)] \quad (6)$$

where the distinction between the two manganese neighbors, which is unnecessary in the paramagnetic state, has been omitted and where \perp and \parallel refer to the orientation with respect to H_0 of the radius from manganese to the fluorine nucleus whose resonance is being observed. These equations reflect the fact that for $H_0 \parallel [001]$ there are two fluorines in the unit cell whose σ bonds to the manganese ion are perpendicular to H_0 and one fluorine whose σ bonds are parallel, where we use σ bonds to mean the interaction between the ions symmetrical about the internuclear radius. The numerical values of the dipole field for these two sites for the particular case of H_0 in the (110) plane, which corresponds to the measurements in Fig. 3 and Fig. 4, are

$$H_{\parallel}^D/H_0 = -2H_{\perp}^D/H_0 = 0.3418\chi_m(3\cos^2\theta - 1) \quad (7)$$

where θ is the angle between H_0 and $[001]$. We are fortunate in that all three measurements⁷ of χ_m at 298°K have a total spread of only 3.5% so that at this temperature the value of $\chi_m = (10.2 \pm 0.2) \times 10^{-3} \text{ cm}^3 \text{ mole}^{-1}$ includes a generous limit of error. Before substituting these values in Eqs. (5) and (6) we will rewrite those equations so as to make the best use of the experimental accuracies.

$$(Ng\beta g_N\beta_N/\chi_m)(\alpha_{\parallel} - \alpha_{\perp} + 3H_{\perp}^D/H_0) = 6(A_\sigma - A_\pi) \quad (8)$$

$$(Ng\beta g_N\beta_N/\chi_m)(\alpha_{\parallel} + 2\alpha_{\perp}) = 6A_s. \quad (9)$$

¹⁴ M. Tinkham, Proc. Roy. Soc. (London) **A236**, 535, 549 (1956).

From the measurements shown in Fig. 2 it can be determined that at 298°K

$$\begin{aligned}\alpha_{11} &= (2.970 \pm 0.02) \times 10^{-2}; \\ \alpha_1 &= (1.852 \pm 0.02) \times 10^{-2}\end{aligned}\quad (10)$$

and $H_1^D/H_0|_{298^\circ} = -0.349 \times 10^{-2}$ where we use the room temperature data because the susceptibility errors should be smallest in the vicinity of 298°K. Substituting these values in Eq. (8) and Eq. (9) we find

$$\begin{aligned}A_s &= (16.26 \pm 0.4) \times 10^{-4} \text{ cm}^{-1} \\ (A_\sigma - A_\pi) &= (0.17 \pm 0.1) \times 10^{-4} \text{ cm}^{-1}\end{aligned}\quad (11)$$

where the accuracy of each of these quantities reflects the possible errors of $\pm 2\%$ in the susceptibility and $\pm 1\%$ in the experimental measurements. The errors in the susceptibility cause a larger fractional uncertainty in the $(A_\sigma - A_\pi)$ than in A_s because they introduce fractional errors into $3H_1^D/H_0$ which is a large quantity compared to its difference from $(\alpha_{11} - \alpha_1)$. If we convert these measured values of the hyperfine interaction to spin densities in the $2s$ and $2p$ orbitals of F^- we have, using the values of the hyperfine interaction given by Moriya⁴

$$\begin{aligned}f_s &= (0.52 \pm 0.02) \times 10^{-2} \\ (f_\sigma - f_\pi) &= (0.18 \pm 0.1) \times 10^{-2}\end{aligned}\quad (12)$$

where f_s , f_σ , and f_π are the fractions of unpaired spin in $2s$, $2p_\sigma$, and $2p_\pi$ orbitals. It is interesting to compare these values with the published values¹ of hyperfine interaction measured in MnF_2 in which

$$\begin{aligned}A_s^I &= (15.4 \pm 0.3) \times 10^{-4} \text{ cm}^{-1} \\ A_s^{II} &= (16.2 \pm 0.3) \times 10^{-4} \text{ cm}^{-1} \\ A_\sigma^I - A_\pi^I &= (0.2 \pm 0.3) \times 10^{-4} \text{ cm}^{-1} \\ A_\sigma^{II} - A_\pi^I &= (0.4 \pm 0.3) \times 10^{-4} \text{ cm}^{-1}\end{aligned}\quad (13)$$

and where we have used the analysis of Keffer, Oguchi, O'Sullivan, and Yamashita.¹⁵ The weighted average of the two values of A_s^I and A_s^{II} , which refer to the two different $Mn^{++}-F^-$ bonds, is¹ $15.7 \pm 0.3 \times 10^{-4} \text{ cm}^{-1}$ while the average of the two values of $(A_\sigma - A_\pi) = 0.3 \pm 0.3 \times 10^{-4} \text{ cm}^{-1}$. The isotropic interaction agrees with the values observed in $KMnF_3$ to within the experimental error while the anisotropic interaction also agrees in that to a first approximation $(A_\sigma - A_\pi)$ is small and not much larger than the experimental error. However in $KMnF_3$ where there are fewer parameters, in fact there are only two as opposed to six in MnF_2 , we have determined without making simplifying assumptions that $(A_\sigma - A_\pi)$ is only very slightly larger than the experimental error.

Let us examine the origin¹⁵⁻¹⁹ of these shifts in more

detail. In our original paper on MnF_2 ¹ we interpreted the hyperfine interactions in terms of unpaired spins in antibonding molecular orbitals. It has been shown that only when the molecular orbitals are orthogonal is this approach proper and equivalent^{15,19} to considering joint effects of the Pauli distortion and coulombic interactions. If the molecular orbital bonding and antibonding orbitals are not chosen to be orthogonal,^{15,17,19} then the matrix element of the hyperfine interaction involves nonvanishing cross terms between different states. We shall continue to use the molecular orbital approach bearing in mind the need for orthogonalized functions in order to simplify the interpretation of the experiments. It is not necessary to write out the complete orthogonalized set of molecular orbitals for the O_h environment because they are available.¹⁷ However the pertinent aspects can be represented in terms of a two center model of $Mn^{++}-F^-$. The molecular orbital wave functions are

$$\begin{aligned}\varphi_b &= \gamma\psi_{Mn} + \psi_F \\ \varphi_a &= \psi_{Mn} - \sqrt{f}\psi_F\end{aligned}\quad (14)$$

where the orthogonalization requires that

$$\sqrt{f} = \gamma + s \quad (15)$$

where

$$s = \langle \psi_{Mn} | \psi_F \rangle \quad (16)$$

and \sqrt{f} is the amount of s or p character admixed in the antibonding orbital. Notice that in the absence of any admixture of metal ion wave function into the bonding orbital, or $\gamma=0$, there still will be an unpaired spin in the antibonding orbital. This contribution has been called the Pauli distortion^{15,16,18} and arises from the nonorthogonality of the atomic orbitals used as starting functions. The second contribution to \sqrt{f} , described by γ , is the energy term which describes how the original atomic orbitals are changed by the Coulomb interactions in the solid.

Keffer¹⁵ *et al.* have calculated f_s and f_σ for the $Mn^{++}-F^-$ bond distances in MnF_2 which are only a few hundredths of an angstrom larger than the 2.09 Å found in $KMnF_3$. They concluded that $f_s \sim 0.36 \times 10^{-2}$ and $f_\sigma \sim 1.0 \times 10^{-2}$. The discrepancy between f_s calculated and observed is not serious considering the difficulty of the calculation. However the large value of f_σ compared with the small value observed indicates there are large p_π contributions which cannot be ignored. In order to show the relative magnitudes of p_σ and p_π contributions we have plotted the appropriate atomic orbitals in Fig. 7. The energy terms, i.e., contributions to γ , are not necessarily equal for p_σ and p_π interactions, however a comparison of the overlaps of p_σ and $p_\pi F^-$ orbitals with the suitable $Mn^{++} 3d$ orbitals provides an indication of the relative sizes of these two

¹⁵ F. Keffer, T. Oguchi, W. O'Sullivan, and J. Yamashita, Phys. Rev. **115**, 1553 (1959).

¹⁶ A. Mukherji and T. P. Das, Phys. Rev. **111**, 1479 (1958).

¹⁷ R. G. Shulman, Am. Soc. Metals (Cleveland, Ohio, 1959), p. 56.

¹⁸ B. S. Gourary and F. J. Adrian, Phys. Rev. **105**, 1180 (1957).

¹⁹ W. Marshall (private communication); W. Marshall and R. N. Stuart (to be published).

interactions. In Fig. 7 we have plotted the fluoride ion $2p$ functions using Slater functions of the form

$$\psi(2p_z) = 5.16r \cos\theta e^{-2.42r} \quad (17)$$

where r is in atomic units of 0.529 Å. For the fluoride ion the Slater function has been shown¹⁶ to be very close to the more accurate Hartree-Fock function. For the Mn^{++} $3d$ orbitals however it is necessary to use the Hartree-Fock functions. We have used the following expressions given by Mukherji and Das¹⁶

$$\begin{aligned} \psi(3d_{z^2}) &= (5/\pi)^{1/2} (3 \cos^2\theta - 1) r^2 (0.11148e^{-1.4711r} \\ &\quad + 8.743e^{-2.683r} + 68.29e^{-5.622r}) \\ \psi(3d_{xz}) &= (15/4\pi)^{1/2} r^2 \sin\varphi \cos\varphi (0.11148e^{-1.4711r} \\ &\quad + 8.743e^{-2.683r} + 68.29e^{-5.622r}). \end{aligned} \quad (18)$$

These functions are plotted in two parts. In Fig. 7(a) we present the Mn^{++} ($3d_{xz}$) function and the $2p_x$ function of the fluoride ion. These are the overlaps of the π bond. The σ bond overlap is presented in Fig. 7(b). A comparison of the two overlaps is interesting because it shows that the π bond overlap is of the same order of magnitude as the σ bond. This near equality is of course helped by the fact that the π bond has two lobes, only one of which is illustrated. The large value of the π overlap was pointed out to us by W. Marshall¹⁹ who had calculated these overlaps numerically. Marshall has included the energy terms of the electron cloud distortion, represented in Eq. (15) by γ , in the overlap term s by using an expanded version of

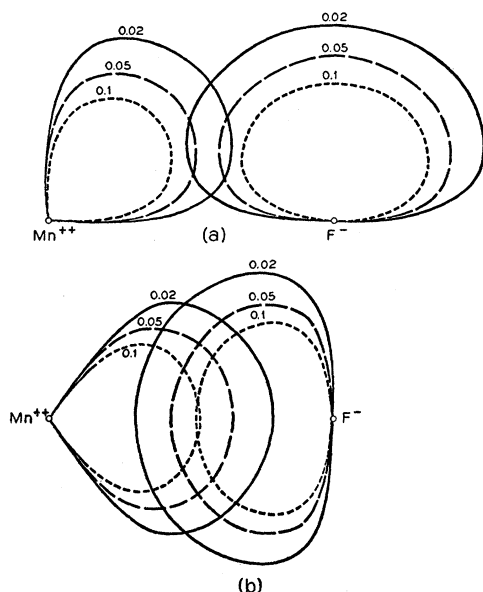


FIG. 7. (a) Contour lines of Hartree-Fock $3d_{xz}$ orbitals of Mn^{++} as described by Eq. (18) are shown overlapping the $2p_x$ Slater function of the F^- ion given by Eq. (17). These orbitals are both antisymmetric with respect to the horizontal axis so that this plot represents only one half of the interaction. The two nuclei are located 3.95 atomic units apart corresponding to 2.09 Å. (b) Similar plot of contour lines of the $3d_{z^2}$ orbital and the $2p_z$ F^- ion orbital.

the Mn^{++} ion Hartree-Fock wave functions. In this way the overlap, when calculated, should equal the amount of admixture in the antibonding molecular orbital or $\sqrt{f=s'}$ is the overlap of the expanded Mn^{++} ion functions. These overlaps have been calculated by Marshall for MnF_2 as

$$\langle 3d_{z^2} | p_z \rangle^2 = 0.74 \times 10^{-2} = f_\sigma$$

and

$$\langle 3d_{xz} | p_x \rangle^2 = 0.28 \times 10^{-2} = f_\pi.$$

It can be seen that $(f_\sigma - f_\pi) = 0.46 \times 10^{-2}$ from this calculation which is larger than the experimental value of $(0.18 \pm 0.1) \times 10^{-2}$. Whether these results indicate the need for considering preferential expansion of the π orbitals with respect to the σ cannot be definitely stated at this time. It is expected that our²⁰ investigations of single crystals of NiF_2 and KNiF_3 which are underway will indicate the strength of the σ interaction alone since in the nickel salts with a $3d^8$ configuration of Ni^{++} ion only σ -bond electrons contribute to the hyperfine interactions. When this information is available these KMnF_3 results will be reconsidered in more detail.

In our abstract⁹ on KMnF_3 we reported an erroneous value of $(A_\sigma - A_\pi) = 1.27 \times 10^{-4} \text{ cm}^{-1}$. This arose from an error in the dipole sum which has been corrected as a result of a conversation with J. M. Mays. In order to check this we have performed the dipole sum for the near neighbors by hand and found it to converge on the machine calculations. Following our abstract⁹ Ogawa and Yokozawa²¹ reported the results of their electron spin resonance experiments on Mn^{++} as a dilute impurity in KMgF_3 . They obtain for the fluoride ion interactions the values $A_s = (18.2 \pm 0.9) \times 10^{-4} \text{ cm}^{-1}$ and $(A_\sigma - A_\pi) = (1.1 \pm 0.9) \times 10^{-4} \text{ cm}^{-1}$. Their value for the anisotropic hyperfine interaction agrees with our value of $(A_\sigma - A_\pi) = 0.17 \pm 0.1 \times 10^{-4} \text{ cm}^{-1}$ only by including the extreme limit of error of both experiments whereas the isotropic contribution is definitely larger than our value of $A_s = (16.26 \pm 0.4) \times 10^{-4} \text{ cm}^{-1}$. Another interesting comparison, unfortunately only of the isotropic part of the interaction, is found²² in a paper by van Wieringen in which he measured the electron resonance of Mn^{++} as a dilute impurity in a number of different diamagnetic host crystals. One of these crystals was KMgF_3 and a pattern of five lines was observed for each of the six components arising from Mn^{55} hyperfine interactions. These five lines in the powdered sample are undoubtedly the five strong central lines of the seven line spectrum expected from hyperfine interactions with the fluorine nuclei. If we assume that Fig. 2 of that paper is drawn to scale we can measure $A_s = 18.5 \times 10^{-4} \text{ cm}^{-1}$ which agrees with the value reported by Ogawa and Yokozawa.²¹

²⁰ R. G. Shulman (to be published).

²¹ S. Ogawa and Y. Yokozawa, J. Phys. Soc. Japan **14**, 1116 (1959).

²² J. S. van Wieringen, Discussions Faraday Soc. **19**, 118 (1955).

These values of the isotropic interaction reveal the influence of interatomic distance upon the s electron admixture. In KMnF_3 the $\text{Mn}^{++}-\text{F}^-$ distance is 2.095 ± 0.003 Å while in KMgF_3 the $\text{Mg}^{++}-\text{F}^-$ distance is 1.993 ± 0.002 Å. We would like to show how the two values of A_s in the different salts can be used to determine the $\text{Mn}^{++}-\text{F}^-$ distance in the mixed crystal. The strong dependence of A_s upon separation has been shown by Kushida and Benedek²³ who applied hydrostatic pressure to MnF_2 while measuring the fluorine resonance frequency. They were able, by using the theory¹⁹ discussed above, to relate these changes to the variation of overlap with distance as calculated by Marshall and Stuart. The same calculation can be applied to the $\text{KMgF}_3:\text{Mn}$ system to determine the $\text{Mn}^{++}-\text{F}^-$ distance in this crystal. It is necessary to extrapolate the calculations as the values are only given in the range of internuclear separation from 2.14 Å to 2.10 Å. The plot of fraction s character vs distance gives a straight line with a slope at 2.10 Å of $df_s/dr = 0.18/\text{angstrom}$. We determine from the A_s values that in KMnF_3 , $f_s = (0.518 \pm 0.02)\%$ while in $\text{KMgF}_3:\text{Mn}^{++}$, $f_s = (0.580 \pm 0.03)\%$ where we have used the relation $f_s = 3.184A_s$ which is based upon the values given by Moriya.⁴ The difference between these two values of f_s is $(0.062 \pm 0.035)\%$ which is equivalent to the $\text{Mn}^{++}-\text{F}^-$ distance in $\text{KMgF}_3:\text{Mn}^{++}$ being (0.033 ± 0.018) Å shorter than in KMnF_3 . This value of 2.062 ± 0.018 Å is intermediate between that observed in the two salts corresponding to an intermediate degree of distortion as one would expect. More accurate calculations and measurements can be made so that one can hope to obtain the internuclear separations in mixed crystals with greater accuracy by this method.

LINE WIDTHS AND SHAPES

The Lorentzian shape lines coupled with our inability to saturate them indicate that the resonances are exchanged narrowed. Moriya⁴ has calculated the widths for this mechanism and has shown that one expects

$$\frac{1}{T_2} = \left(\frac{\pi}{2}\right)^{\frac{1}{2}} \frac{S(S+1)}{3\hbar^2\omega_e} \sum_{i=x,y,z} (\cos^2\theta_i + \frac{1}{2}\sin^2\theta_i) A_i^2 \quad (19)$$

where S is the electronic spin and ω_e the exchange frequency in these dense paramagnetics. The sum is over the three principle axes of the hyperfine interaction while θ_i is the angle between the i th principle axis with combined dipole and hyperfine interaction A_i and the direction of H_0 . A feature of this expression is the contribution of the off-diagonal terms to the line width. Using Eq. (19) we obtain for the two lines

$$1/T_2 = 3.42 \times 10^{18}/\omega_e \quad (20)$$

and

$$1/T_2 = 2.67 \times 10^{18}/\omega_e$$

for the lines designated as parallel and perpendicular in Eq. (6) and Eq. (5), respectively. The ratio of these two theoretical widths is 1.28 while the observed ratio is 1.32 ± 0.1 . It is worth noting that if instead of Eq. (19) we were to assume that only the secular terms contribute to the relaxation, the line width would be proportional to the square of the hyperfine interactions. Then the ratio would be 2.6. Thus we see the experimental confirmation of the importance of considering the off diagonal contributions.

If we confine our attention to the broader of the two lines, considering that its width is more reliable since it is less subject to other sources of line broadening, we can calculate that $\omega_e = 6.2 \times 10^{12} \text{ sec}^{-1}$. This same quantity can be estimated from T_N by the relation

$$\omega_e = \frac{kT_N}{\hbar} \left(\frac{6}{zS(S+1)} \right)^{\frac{1}{2}} \quad (21)$$

we find that for $T_N = 88^\circ$ and $z=6$ the value of ω_e is 3.9×10^{12} . Considering the assumptions of Eq. (21) this agreement must be regarded as satisfactory.

CONCLUSIONS

1. A change in the fluorine nuclear magnetic resonance pattern in the vicinity of 88.5°K is consistent with an antiferromagnetic transition occurring at this temperature.

2. The shifts of the F^{19} resonance enable us to calculate the isotropic and anisotropic hyperfine interactions between this nucleus and the electrons. These are $A_s = (16.26 \pm 0.4) \times 10^{-4} \text{ cm}^{-1}$ and $(A_\sigma - A_\pi) = (0.17 \pm 0.10) \times 10^{-4} \text{ cm}^{-1}$ respectively corresponding to $f_s = (0.52 \pm 0.02) \times 10^{-2}$ and $(f_\sigma - f_\pi) = (0.18 \pm 0.1) \times 10^{-2}$ which are the admixture of magnetic electrons in fluoride ion orbitals.

3. The small value of $(f_\sigma - f_\pi)$ compared to f_s is partially explained by a cancellation of the σ -electron contribution by the π electron's contribution.

4. The difference between the isotropic coupling constant of $A_s = 16.26 \times 10^{-4} \text{ cm}^{-1}$ and the value observed in $\text{KMgF}_3:\text{Mn}^{++}$ is explained on the basis of the change of coupling constants with bond distances. We determine that in $\text{KMgF}_3:\text{Mn}^{++}$ the $\text{Mn}^{++}-\text{F}^-$ distance is intermediate between the $\text{Mg}^{++}-\text{F}^-$ distance and the $\text{Mn}^{++}-\text{F}^-$ distance in KMnF_3 .

ACKNOWLEDGMENTS

Dr. P. W. Anderson, Dr. W. Marshall, and Dr. J. M. Mays have all helped us by crucial suggestions. Mr. B. J. Wyluda's assistance in the experiments is most gratefully acknowledged. We are particularly indebted to Dr. N. Elliott of Brookhaven National Laboratory and Dr. R. L. Martin of the University of New South

²³ T. Kushida and G. Benedek, Bull. Am. Phys. Soc. 4, 183 (1959) and (private communication).

Wales for communicating to us their susceptibility measurements prior to publication. A conversation with Dr. A. M. Clogston stimulated us to develop the wave functions in the Appendix.

APPENDIX

It is not obvious that the description of the system in terms of the orthogonalized ligand field orbitals is perfectly suitable for explaining the experimental observations. After all—the measurements are made on the fluorine nucleus and it is the total spin density in one fluoride ion, with the possibility of interactions between the fluoride orbitals, that should be considered. This question has been discussed by Keffer¹⁵ *et al.* in terms of the fluoride ions in MnF_2 . They assume two different models of interaction. The first, which they call the independent bonding model, is what we have assumed in the text. In this approximation one considers there to be two separate contributions to the fluorine hyperfine interaction from the two neighboring manganese ions. The interactions of the individual fluorine orbitals with these neighbors are independent of each other.

As a second model they consider the effects of hybridization of the fluorine orbitals. They recognize this is a suitable approximation only in the event of strong covalent bonding which they do not expect in these fluorides. As proof that the hybridized orbitals do not contribute appreciably to the electronic configuration they calculate the hyperfine interactions on this interdependent basis, i.e., where relative s and p contributions depend upon the bond angles, and show that the results do not agree with the values measured for the individual bonds by Tinkham for Mn^{++} in ZnF_2 . As long as the energy considerations do not encourage the formation of strong covalent bonds hybridization is not important. However we have become accustomed to think of certain geometrical arrangements in terms of directed valences and the

consequential hybridization. For example, a linear configuration like $\text{Mn}^{++}-\text{F}^--\text{Mn}^{++}$ immediately suggests s - p hybridization. Therefore it seems necessary to show that LCAO molecular orbitals can be written for this three-centered configuration which are basis functions of the irreducible representations of the point group D_{4h} . It can be shown that the orthonormal linear combinations of fluoride ions $2s$ and $2p$ functions (ψ_s and ψ_p) with the manganese ion $3d$ orbitals (ψ_1 and ψ_2) which describe the sigma bonds are:

$$\begin{aligned}\varphi^{(1)} &= [1+4aS_s+2a^2]^{-\frac{1}{2}}[\psi_s+a(\psi_1+\psi_2)] \\ \varphi^{(2)} &= [1+4bS_p+2b^2]^{-\frac{1}{2}}[\psi_p+b(\psi_1-\psi_2)] \\ \varphi^{(3)} &= [2-4cS_s+c^2]^{-\frac{1}{2}}[c\psi_s-(\psi_1+\psi_2)] \\ \varphi^{(4)} &= [2-4dS_p+d^2]^{-\frac{1}{2}}[d\psi_p-(\psi_1-\psi_2)]\end{aligned}\quad (\text{A-1})$$

where

$$c = \frac{2(a+S_s)}{1+2aS_s}, \quad d = \frac{2(S_p+b)}{1+2bS_p}$$

and where

$$S_s = \int \psi_1 \psi_s d\tau = \int \psi_2 \psi_s d\tau$$

$$S_p = \int \psi_1 \psi_p d\tau = - \int \psi_2 \psi_p d\tau.$$

These three-center molecular orbitals include the same degrees of freedom as the independent bonding model used in the text as the basis for Eq. (2). The antibonding orbitals $\varphi^{(3)}$ and $\varphi^{(4)}$ contain the unpaired spins responsible for the hyperfine interactions observed, while similar orbitals can be written for the π electron interactions. The admixture parameters c and d are related to the parameters of Eq. (12) in the text by the relationship

$$c^2 = 2f_s \quad (\text{A-2})$$

and

$$d^2 = 2f_p.$$